APPLICATION OF MEMORY-BASED DIGITAL FILTERING TO HIGH-SPEED DIGITAL RADIO

Curtis A. Siller, Jr., and Walter Debus, Jr.

Curtis A. Siller, Jr., *and* ***Walter Debus, Jr.,*** *are with AT&T Bell Laboratories in Andover, Massachusetts. Mr. Siller is a distinguished member of technical staff and an AT&T Bell Laboratories fellow in the Digital Cross-Connect and Multiplex Systems Engineering Department. He works on synchronous optical network transmission and specifications of high-functionality multiplex equipment. He has B.S., M.S., and Ph.D. degrees in E.E. from The University of Tennessee, Knoxville. He joined AT&T in 1969. Mr. Debus is a supervisor in the Digital Terminals and Microwave Technology Department. He works on developing specialized products such as restoration test equipment for AT&T Network Services Divison. He has an M.S.E.E. degree from Lowell University, Lowell, Massachusetts. He joined AT&T in 1969.*

Memory-based digital filtering is considered in the context of high-speed (greater than 15 Mbaud) radio systems, where it finds application as an accurate and rapid approach to synthesizing band-limited data signals for transmission over Nyquist channels. Following brief comments regarding the basic circuit architecture, feasibility models for 16- and 64-QAM 90-Mb/s operation are experimentally evaluated. Performance is found to be consistent with digital radio objectives and superior to sophisticated analog designs.

Introduction

High-capacity digital radio systems rely on band-limiting filters that afford minimal intersymbol interference (ISI) while making efficient use of the available transmission spectrum. The most common approach to this challenge is to make use of lumped-element analog filters. This technology requires lengthy development intervals that often entail sophisticated analytic and empirical design methods. Moreover, these analog filters are costly in that they require individual factory tuning during manufacture. Where analog finite-impulse-response (FIR) filters incur similar limitations, digital FIR filters with multipliers trade off inherent reproducibility and ease of realizability against increased expense and power consumption, especially for high-speed [greater than 15 Mbaud (megabaud)] operation. Older binary transversal filters (BTFs), with resistive register networks, share many of the limitations of lumped-element FIR filters; newer BTFs or direct-addressing FIR filters rely on discrete summers and can be awkward to fabricate for high-level modulation.

The architecture used here is that of a memory-based filter, wherein addresses defined from the binary bitstream at the transmitter are used to look up precomputed summed outputs that correspond to symbol weighting of a characteristic truncated impulse function. This method has been applied to the design of voiceband modems. Since the symbols of an M-ary signal are themselves defined by the binary stream at the transmitter, the same technique is well suited to contemporary multilevel quadrature amplitude modulation (QAM) radio systems.[1,2]

The scope of this work includes a brief review of the conceptual basis and presentation of an analytic spectral model appropriate to digital radio. These are followed by a more detailed discussion of issues, performance attainments, and design considerations relevant to the attainment of complementary spectra for megabaud radio transmission. The transmitter filter is complementary in the sense that, for the present applications, the transmitter filter matches, in amplitude and phase, a receiver filter, so as to provide an overall baseband channel that is nearly *Nyquist*, i.e., free of intersymbol distortion. Approximately half the baseband Nyquist spectral shaping appears at the transmitter; the other half is at the receiver. It should be noted that, though the present focus is on transfer functions band-limited to less than the baud frequency f_b, the technique has been described for arbitrary spectral shaping of M-ary signals.[3]

The remainder of this paper is divided into two sections. The first briefly presents the fundamental principles. The second discusses performance attainments, notably theoretical and measured spectra, theoretical and measured digital eyes, and measured probability-of-error data. The error rate data are presented in the formats of bit error rate (BER) versus signal-to-noise ratio (S/N) for single-rail filtering and of equipment signature curves for QAM operation. The performance data of the second section is further divided into two subsections, corresponding to 4- and 8-level signals appropriate to 16 and 64 QAM, respectively. As we show, the number of discrete amplitude levels in the transmitted data stream intimately affects the filter implementation and performance capability.

Panel 1. Acronyms in This Paper

ARF	analog receiver filter
ATF	analog transmitter filter
BER	bit error rate
BTF	binary transversal filters
CPU	central processing unit
D/A	digital-to-analog
DF	digital filter
FCC	Federal Communications Commission
FIR	finite impulse response
IF	intermediate frequency
ISI	intersymbol interference
GPOP	General-Purpose Optimization Program
LPF	low-pass filter
PEC	peak digital eye closure
QAM	quadrature amplitude modulation
RF	radio frequency
ROM	read-only memory
S/P	serial-to-parallel
SR	shift register

Fundamental Principles

The memory-based digital filter is based on a time-domain representation for a transmitted data stream made up of shaped M-ary pulses, namely

$$s(t) = \sum_{n=-\infty}^{\infty} a_n p(t - nT) \qquad (1)$$

where each transmitted symbol a_n describes one of M discrete amplitude levels, $p(t)$ is the impulse response of a spectral shaping function $P(f)$; and T is the interval between the transmission of successive data symbols. For digital radio systems, $P(f)$ is band-limited to $f \leq 1/T$ and implies an infinite impulse response. Nevertheless, it is often the case that $p(t)$ decays quickly, a situation that applies to the raised-cosine, half-Nyquist transfer functions important to this study. Furthermore, the band-limited nature of the transmitted signal, in conjunction with the Nyquist sampling requirement, indicates that both $p(t)$ and $s(t)$ are uniquely characterized by $T/2$-spaced samples of the transmitted data stream.

The observations of suitable impulse windowing and appropriate sampling are the basis for memory-based digital filtering. The architecture depicted in Figure 1 illustrates the case of a 4-level signal, for which the

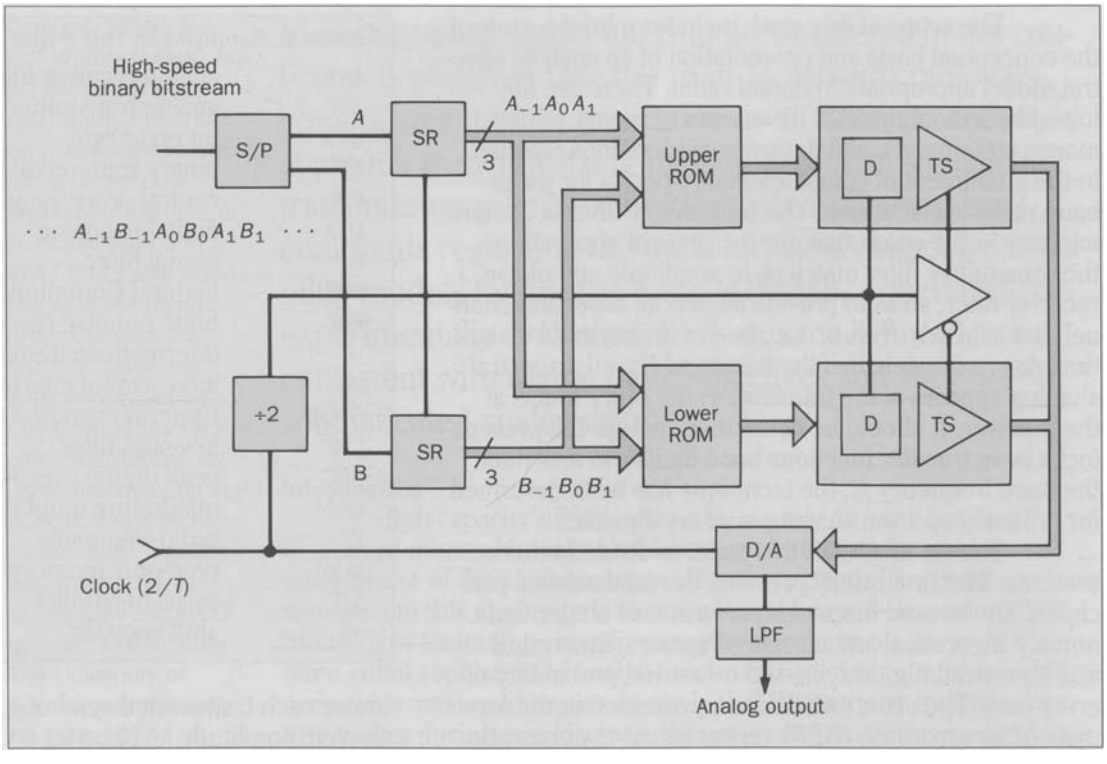

Figure 1. Functional description of the memory-based digital filter, corresponding to a 4-level signal with characteristic pulse spanning 2.5 T and requiring a three-symbol address. The filter processes the high-speed binary bitstream input to form an analog output.

impulse response is truncated to span two symbols. Each transmitted symbol requires two bits (A, B) embedded in the high-speed binary stream

$$\cdots A_{-1}\ B_{-1}\ A_0\ B_0\ A_1\ B_1 \cdots$$

The serial-to-parallel (S/P) converter transfers the binary data to two parallel rails, with binary data $\cdots A_{-1}\ A_0\ A_1 \cdots$ and $\cdots B_{-1}\ B_0\ B_1 \cdots$. Using a T-clocked (synchronous) tapped delay line made up of shift registers (SRs), the symbol-rate data is passed in parallel to address each of two read-only memories (ROMs). This memory pair can be viewed as providing the two outputs required within each symbol period, as stipulated by the Nyquist sampling condition. Observe that Figure 1 also includes a digital-to-analog (D/A) converter and low-pass filter (LPF). The D/A converter operates at the $2/T$ rate and introduces $[\sin(\pi fT/2)]/(\pi fT/2)$ spectral shaping, denoted here as $G(f)$ and commonly referred to as an *aperture effect*. An LPF is provided to minimize aliasing by removing the periodic portion of the output spectrum.

Memory Requirements. Filter memory requirements are closely tied to the transmitter pulse length and the number of levels in the M-ary signal. If the truncated pulse requires $JT/2$-spaced samples, the address length for each ROM in Figure 1 is $[(\log_2 M)(J/2)]$ bits and there are $2 \exp[(\log_2 M)(J/2)]$ addressable memory locations. It is also apparent that, in a filter of this type, memory demands can quickly become

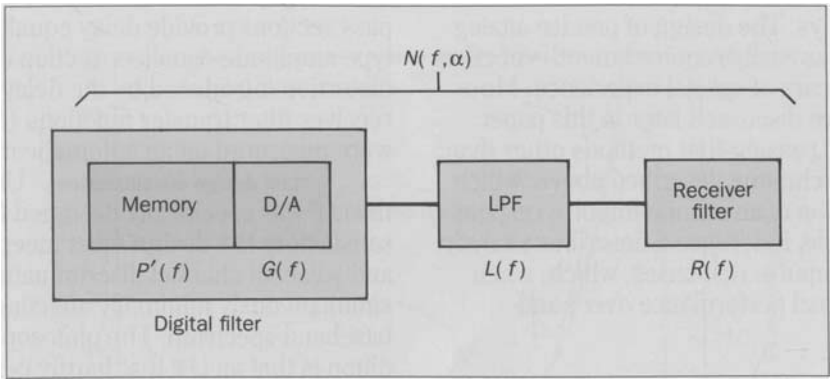

Figure 2. Baseband communication system. Spectral components of the digital filter, an external low-pass filter, and a receiver filter. The external LPF is usually analog.

prodigious. However, it has been noted that addresses can be segmented into smaller units, resulting in "partial sum" ROMs with intermediate adders.[4] For example, an address made up of 27 bits and dictating one ROM with 134,217,728 memory locations is equivalent to three ROMs, each with 512 addressable locations, and two intermediate adders. In practice, care must be taken to balance address segmentation with the number of ROM and summer units, since they directly affect circuit complexity.

Spectral Matching. As applied in this work, the transmitter transfer function is spectrally matched to the receiver, with the objective of achieving a raised-cosine Nyquist channel, $N(f, \alpha)$, with a roll-off factor α. Considering the baseband communication system outlined in Figure 2, we have

$$P(f)\,G(f)\,L(f)\,R(f) = N(f, \alpha) \qquad (2)$$

where $P(f)$ is the transfer function stored in digital memory, momentarily assuming that the impulse function is not truncated; $G(f)$ characterizes the aperture effect; and $L(f)$ and $R(f)$ denote transfer functions of the low-pass and receiver filters, respectively. The actual pulse function used to define the stored memory contents, $p'(t)$, is derived by truncating $p(t)$, which is itself obtained from equation (2) after solving for $P(f)$ and performing an inverse Fourier transform.

One approach to assessing the extent to which the transmitter and receiver are accurately matched after truncating $p(t)$ to $p'(t)$ is to first note that the net channel impulse response $w(t)$ is given by

$$w(t) \leftrightarrow W(f) = P'(f)\,G(f)\,L(f)\,R(f) \qquad (3)$$

The peak channel distortion, D_p, can then be determined by minimizing the intersymbol distortion function,

$$D_p = \frac{1}{|w(\tau)|} \sum_{n=-\infty}^{\infty}{}' |w(\tau + nT)| \qquad (4)$$

over the range $-T \le \tau \le T$, where τ is the receiver timing phase and Σ' indicates that the summation excludes the $n = 0$ term. This minimization was carried out using computer programs designed for that purpose, and builds on General-Purpose Optimization Program (GPOP) optimization procedures.[5] The spectral matching approach described above requires that the designer identify a roll-off factor and appropriate range for impulse truncation that meet design objectives. For the two designs described below, the roll-off was close to that of the receiver filter, and the impulse was truncated to span several (4 to 8) symbol periods. Moreover, what empiricism the design method requires is expedited by the fact that $P'(f)$ can be changed within hours, with entire transmitter filter

designs completed in days. The design of precise analog filters for digital radio has easily required months of effort by technical staff with years of special experience. More specific design issues are discussed later in this paper.

We comment in passing that methods other than the spectral matching technique described above, which includes simple truncation of an infinite impulse response, are possible. For example, Reference 6 describes analytic means to derive finite impulse responses, which, when convolved, provide optimal performance over band-limited channels.

Performance Attainments

The previous section reviewed fundamental principles of memory-based filtering as it applies to digital radio. We note that the number of discrete signal levels, M, is an important parameter that could significantly affect filter complexity and performance. This section is consequently subdivided into two subsections, dealing individually with filtering of 4-level and 8-level signals for 16- and 64-QAM transmission, respectively.

Four-Level Spectral Shaping. The first example addresses design issues and performance attainments of a 4-level, 22.631-MHz (megahertz) memory-based filter that spectrally matches transmitter low-pass and receiver half-Nyquist filters. Paralleling the schematic channel of Figure 2, we describe the analog receiver and low-pass filters, followed by comments relating to impulse truncation and spectral issues. The subsection concludes with a discussion of performance characteristics.

Analog Receiver Filter. The analog receiver filter (ARF) was previously designed for a 6-GHz (gigahertz), 90-Mb/s (megabits per second) QAM digital radio system (the AT&T DR6 digital microwave radio system) employing raised-cosine Nyquist filtering with 45-percent roll-off and a 22.63-Mbaud symbol rate.[7] The approximate half-Nyquist ($\approx \sqrt{N(f,\alpha)}$) shaping at the receiver is realized by using a single, bump-type, amplitude equalizer section; stopband requirements are achieved with a seventh-degree, inverse-Chebyshev LPF; and three all-pass sections provide delay equalization. A single valley-type amplitude equalizer section corrects for amplitude distortion introduced by the delay equalizers. The receiver filter transfer functions (amplitude and phase) were measured on an automatic measurement system.

LPF design considerations. Unlike the receiver filter, the LPF was specifically designed for this application. A satisfactory LPF design must meet transmitter emission and adjacent channel discrimination requirements while simultaneously minimally affecting the transmitted baseband spectrum. The philosophy behind this last condition is that an LPF that hardly perturbs the transmitted baseband power spectral density should not significantly affect (for better or worse) the digital peak eye closure. This condition assures that a relatively loose and unsophisticated LPF design will not degrade system performance. To do otherwise—that is, to make the performance of the digital filter critically dependent on a complex analog LPF—would negate the basic motivation for this technological approach: to obviate the need for complicated analog transmitter filters, with their attendant difficulties.

Such a simple LPF can be used in conjunction with half-Nyquist spectral shaping; this is accomplished by placing the LPF cutoff f_c within the half-Nyquist stopband f_{sb}. From basic equations for $N(f,\alpha)$, this is easily shown to be

$$(1 + \alpha)\frac{1}{2T} \leq f_{sb} \leq \frac{1}{T} \tag{5}$$

with $\Delta_{sb} = 1/T - (1 + \alpha) / (2T) = (1 - \alpha)/(2T)$. For the present case, this stopband, sometimes referred to as a *guard band*, extends from 16.4 to 22.6 MHz. The guard band is sufficiently wide that distortion caused by the LPF's amplitude and delay shape near cutoff, partially compensated by spectral matching, only slightly extends into the half-Nyquist shape below $(1 + \alpha)/(2T)$. We have theoretically found[2] that, if the LPF is removed completely, peak distortion is increased by less than 0.0037,

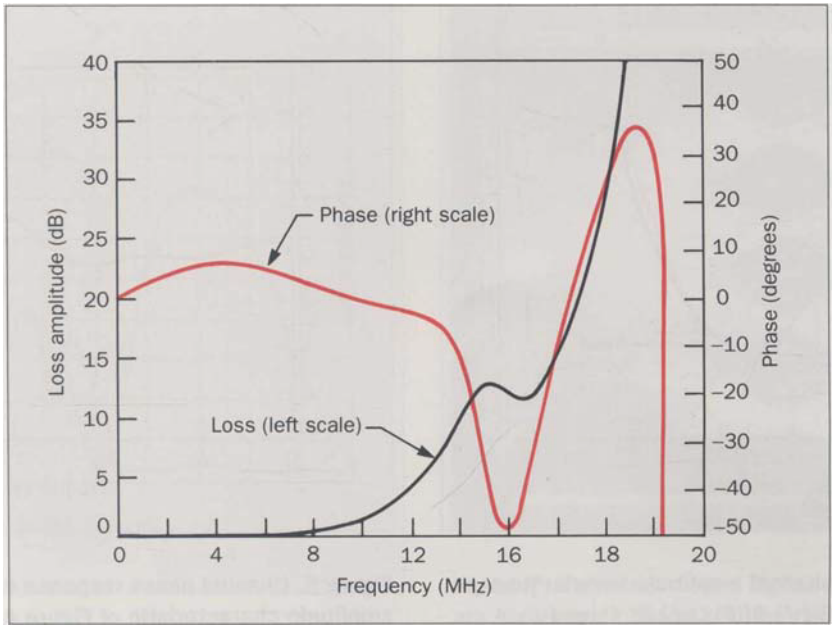

Figure 3. Composite receiver and LPF transfer function $L(f)\,R(f)$, with 0-Hz flat loss and constant delay removed. The analog receiver filter was designed for a 16-QAM radio system; the LPF is a fifth-order Chebyshev filter.

provided $\Delta f_{sb}\,T \geq 0.25$. This condition applies to raised-cosine and half-Nyquist filtering with roll-offs less than 0.5. For roll-offs greater than that, the guard band is proportionately smaller. Minimal performance degradation associated with the LPF is still attainable, though it could place greater demands on the filter design. On the other hand, the larger roll-off corresponds to a wider baseband spectrum and, therefore, a more "compact" impulse response. For the same amount of memory, this usually translates into reduced peak distortion and permits a corresponding relaxation of LPF performance.

The LPF used here is a fifth-order Chebyshev filter designed for 0.025-dB (decibel) peak-to-peak passband ripple. The high-frequency cutoff is selected to occur at 18 MHz; the filter has a single transmission zero at 30 MHz, with a minimum stopband response of –43 dB beyond that point. Measured data reveal that little amplitude or phase shaping appears below the half-Nyquist band at 16.4 MHz. Filter design, fabrication, and experimental characterization were completed in less than a day.

Spectral issues. The composite receiver and LPF transfer function $L(f)\,R(f)$, with 0-Hz flat loss removed, is presented in Figure 3. Using this measured data with equation (2), we form the required synthesizer response, $P(f)\,G(f) = N(f,\alpha)/[L(f)\,R(f)]$, that approaches a full-Nyquist raised-cosine channel when cascaded with the LPF and ARF.

With the measured data of Figure 3 and the functional form for $G(f)$ stated earlier, $p(t)$ is evaluated via an inverse Fourier transform. For this 4-level design, $p(t)$ was approximated by using just nine samples between $-2T \leq t \leq 2.5T$. With $p'(t)$ thus defined, $P'(f)$, the transfer function stored in the synthesizer memory, and then w(t), the overall channel impulse response, are computed. For this relatively coarse impulse truncation, equation (4) predicts a minimum distortion of 0.0297 for $\alpha = 0.42$. (The roll-off factor may be viewed as an inde-

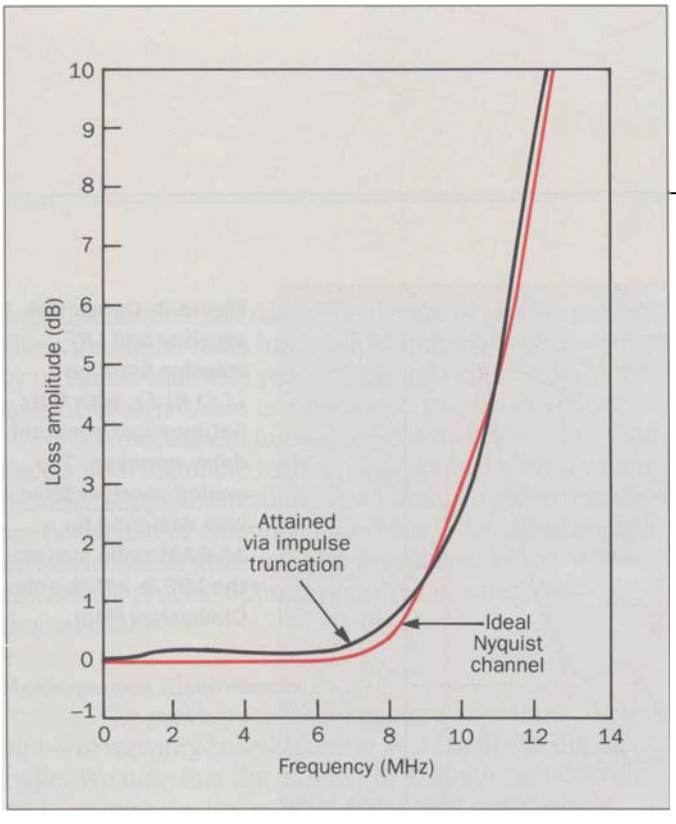

Figure 4. Comparison of channel amplitude transfer functions corresponding to $|P'(f)G(f)L(f)R(f)|$ and $N(f,\alpha = 0.42)$, the former predicated on $f_b = 22.631$ MHz and a pulse spanning 4.5 T.

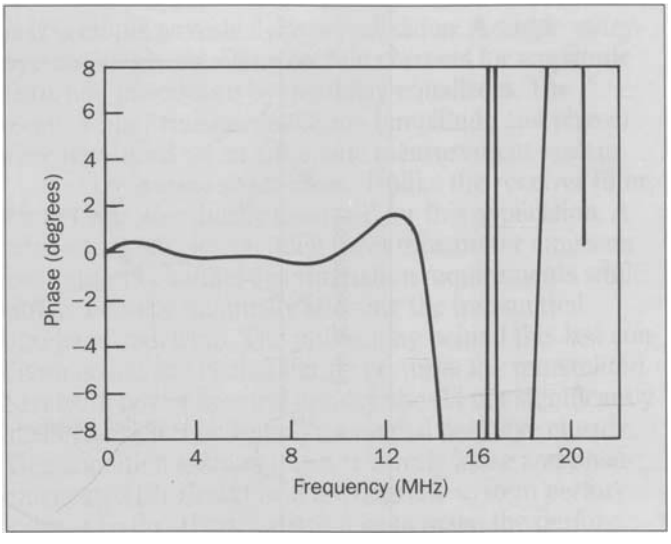

Figure 5. Channel phase response corresponding to the amplitude characteristic of Figure 4.

pendent parameter that, in conjunction with pulse length, can be used to minimize overall channel distortion. However, α cannot be selected in isolation, since it also affects adjacent channel interference and the ability to meet emission mask criteria.) The corresponding peak digital eye closure (PEC), defined by $\text{PEC}_M = D_p(M - 1)$, is 8.9 percent for 4-level signals. This theoretical PEC, which does not include quantization effects associated with the digital circuit realization, is competitive with theoretical eye closures attained using advanced analog filter technology. The effect of quantization noise associated with the finite word length of the ROM outputs is accurately modeled as a peak signal-to-quantization noise ratio with binary coding. From Reference 8, we have

$$(S/N)_{\text{dB}} = 4.8 + 6m \qquad (6)$$

where m is the output word length. With $m = 8$, $S/N = 52.8$ dB and was considered negligible for the 16-QAM application.

For the truncated impulse response described above, in conjunction with the measured data, $L(f)R(f)$, the expected end-to-end channel amplitude transfer function, $|P'(f)G(f)L(f)R(f)|$, was computed for $\alpha = 0.42$. As shown in Figure 4, comparison with the ideal Nyquist response is quite good, considering the relatively short length of the pulse function $p'(t)$. The expected channel phase response is similarly presented in Figure 5 and attests to the relatively flat phase response achievable. (The unusual phase characteristic beyond approximately 14.4 MHz, due to nulls in the corresponding amplitude shape, is of little consequence, since beyond that point the overall amplitude response is down over 20 dB from its 0-Hz level.)

Four-Level Shaping Performance. The preceding remarks primarily deal with theoretical performance

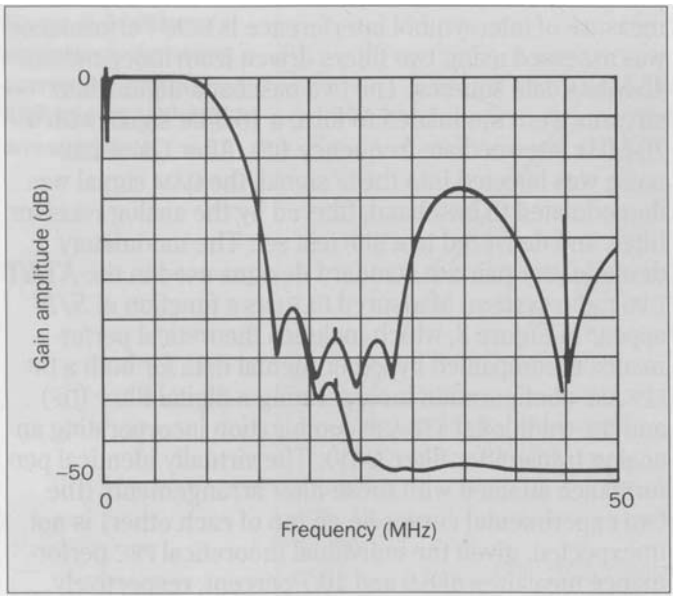

Figure 6. Transmitted amplitude spectrum measured with and without LPF. The LPF affects the baseband spectrum only at high frequency, where the channel response is low anyway.

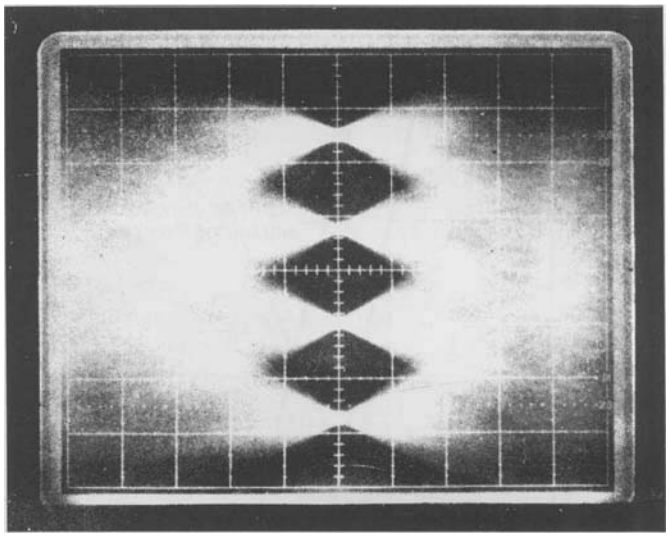

Figure 7. Measured 4-level digital eyes. The eye openings are highly symmetrical and their size agrees closely with that predicted by theory.

measures. Turning attention to the experimental realization, we used the truncated impulse response to compute the signal output for each of 1024 unique addresses in both the upper and lower ROMs. The signals were first scaled so that the maximum output could be represented by an 8-bit word, and then individual outputs were rounded to an 8-bit representation for storage in the filter memory.

Spectra. Using an 8-bit D/A converter, we measured the transmitted amplitude spectrum with and without the LPF; the spectrum appears in Figure 6. Note that the LPF does not begin to affect the baseband spectrum until 20 MHz, where the amplitude response is down over 30 dB. Consequently, the quality of the overall communication channel would probabily be insensitive to manufacturing variations in the assembly of that component. Secondly, the measured response beyond approximately 23 MHz represents the periodic portion of the spectrum. The spectral null near 45 MHz is due to the aperture effect, with the first zero in $|G(f)| = |[\sin(\pi fT/2)]/(\pi fT/2)|$ occurring at $f = 2/T$.

These channel spectra may be considered of secondary interest only; the immediate concern is to provide a raised-cosine channel that is predominantly free of ISI. As noted elsewhere, two of the more relevant measures of channel quality are actually peak digital eye closure and probability-of-error data. These measures are discussed in detail below.

Digital eye closure and BER versus *S/N*. Four-level digital eyes, shown in Figure 7, were measured by using a 45-Mb/s pseudorandom data source. The pronounced symmetry of the eye openings attests to a linear channel phase characteristic, as anticipated from the theoretical

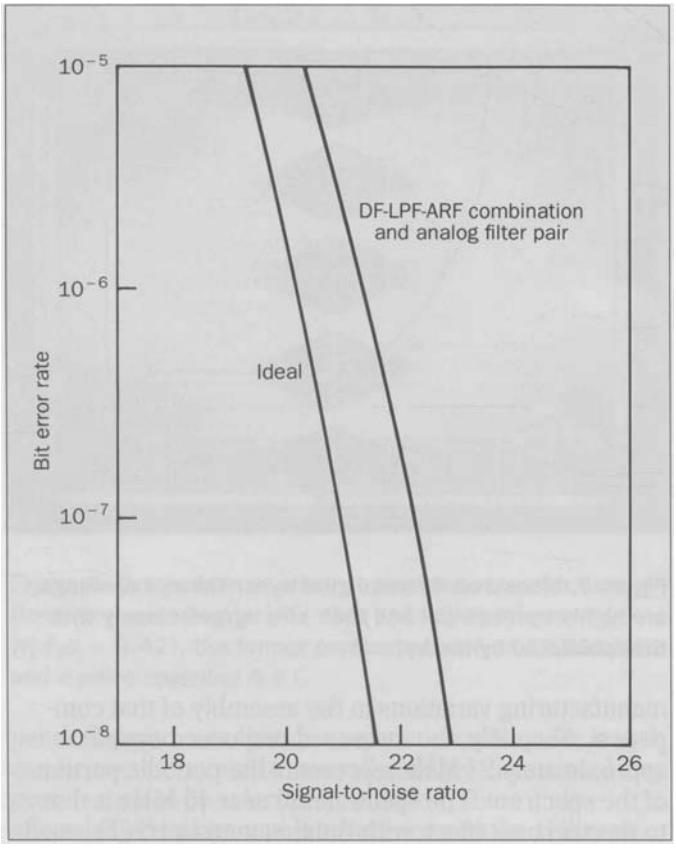

Figure 8. Measured BER versus *S/N* for both ATF-ARF (analog filter pair) and DF-LPF-ARF configurations, with theoretical (ideal performance) data shown for comparison. The ATF-ARF curve is virtually identical to the DF-LPF-ARF curve; the two appear superimposed in this plot.

data of Figure 5. Additionally, the visible eye openings in Figure 7 are approximately 10.7 percent and show good agreement with a theoretical value of 8.9 percent computed from equation (4).

Measured digital eyes afford only a qualitative measure of digital system performance. A more sensitive measure of intersymbol interference is BER. Performance was assessed using two filters driven from independent 45-Mb/s data sources. The two baseband digital data streams were modulated to form a 16-QAM signal with a 70-MHz intermediate frequency (IF). After Gaussian noise was injected into the IF signal, the QAM signal was demodulated to baseband, filtered by the analog receiver filter, and delivered to a BER test set. The modulator/demodulator pair are standard designs used in the AT&T DR6 radio system. Measured BERs as a function of S/N appear in Figure 8, which includes theoretical performance accompanied by experimental data for both a DF-LPF-ARF configuration incorporating a digital filter (DF) and the traditional ATF-ARF combination incorporating an analog transmitter filter (ATF). The virtually identical performance attained with these filter arrangements (the two experimental curves lie on top of each other) is not unexpected, given the individual theoretical PEC performance measures of 8.9 and 10.7 percent, respectively. Additionally, the data presented in Figure 8 should be considered in the following context: the analog filters in the ATF-ARF arrangement are extremely precise and were developed after months of intense development; in contrast, the DF and LPF were both designed in several days. The digital transmitter filter offers the further attributes of inherent reproducibility and a manufacturing cost that is competitive with the analog designs.

Equipment signature curves. As noted in the introduction, equipment signature curves are an especially important performance measure for QAM digital radio applications. The equipment signatures are obtained by stressing a radio system with a two-ray multipath fade, modeled after one used in the widely cited work of Rummler.[9] The equipment signature corresponds to a 10^{-3} BER locus as the fade-notch depth and fade-notch position (relative to the carrier) are varied across the channel band. These signatures do not include noise, but do include degradations associated with modulation/demodulation and carrier and timing recovery. Measured equipment signatures, accurate to ±0.25 dB, are

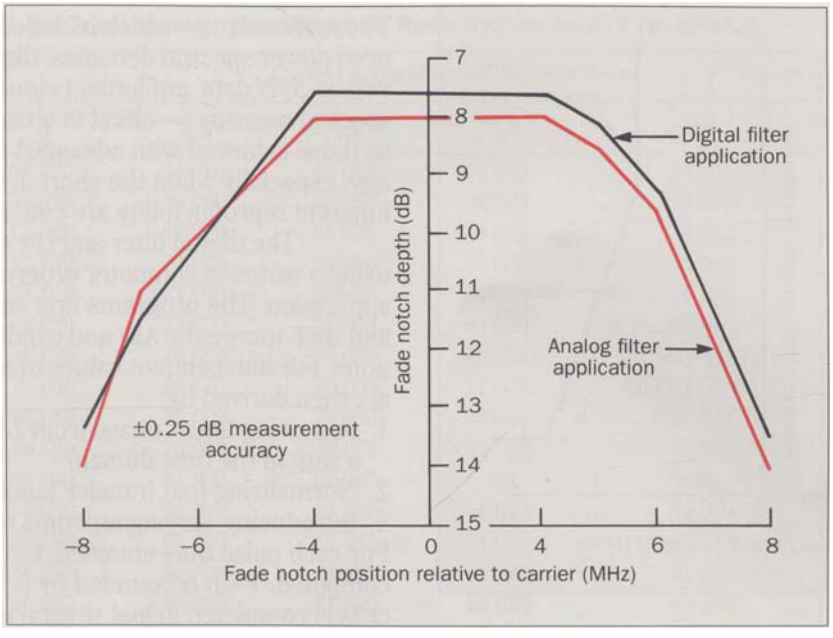

Figure 9. Measured equipment signature curves for both ATF-ARF and DF-LPF-ARF arrangements.

presented in Figure 9 and reveal no significant difference between the DF-LPF-ARF and ATF-ARF arrangements. This observation should again be interpreted in light of previous comments as to relative design effort, development time, and reproducibility of the alternative transmitter filter approaches.

Nonlinear RF spectral spreading. The LPF serves the important functions of limiting the baseband transmitter spectrum while simultaneously preserving the nominally half-Nyquist shape. In digital radio, the transmitted RF signal exhibits the effect of spectral spreading due to nonlinearities introduced during power amplification. To keep the transmitted spectrum within Federal Communications Commission (FCC) emission mask requirements and assure minimal interference with other ("foreign") radio systems, the baseband spectrum must be carefully band-limited.

Measured 1-watt RF power spectral densities [10-kHz bandwidth, 0-dB normalization at a 6.0045-GHz carrier frequency, –47-dB noise floor] for the DF-LPF arrangement appears in Figure 10 with the FCC emission mask requirement.[10] The measurements indicate that the digital filtering scheme meets the emission mask requirement at all frequencies above and below the carrier.

An interesting feature is the lobes in the skirts of the RF transmitted spectrum. The lobes are due to truncation of the impulse response and are analogous to the Gibbs phenomenon in Fourier series. While these lobes evidently meet the emission mask, they could adversely affect the interference environment for other 6-GHz radio systems, particularly if the carrier frequencies have a wide (15- to 30-MHz) offset. The influence of the transmitted RF spectrum on other digital and analog radio systems has been determined by computing the necessary carrier-to-interference (C/I) objectives for operation with the DR6 radio system. (That is, the foreign system carrier power, relative to the DR6 interfering power level, necessary for satisfactory foreign system operation, has been

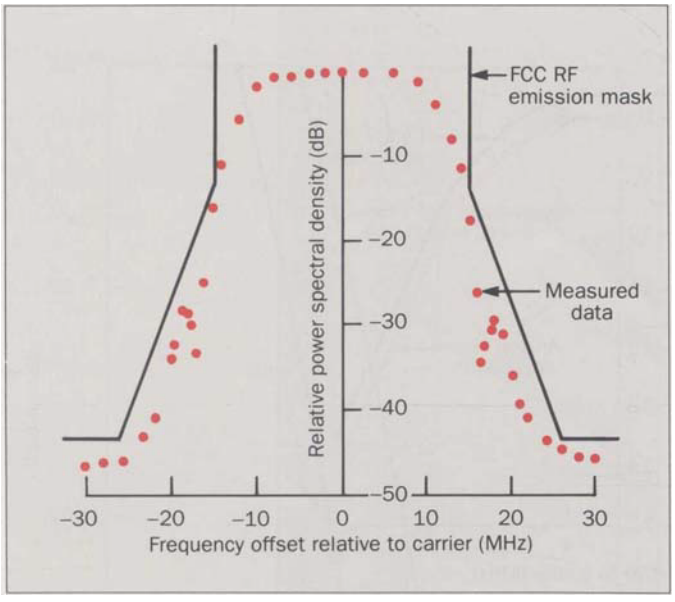

Figure 10. Measured 1-watt RF transmitted power spectral densities for the ATF and DF-LPF filter arrangements.

computed. The lower the C/I objective, the less susceptible a system is to interference from a DR6 system.) The C/I objectives for a variety of radio systems, assuming 0.5- and 1-watt DR6 operation, appear in Table I. For each radio system, the table gives the C/I objective as a function of carrier separation for both ATF and DF-LPF filtering. The data show that the C/I ratios are generally equivalent, particularly for carrier separations of 0 to 22.5 MHz. For a 30-MHz separation, the DF-LPF option tends to establish C/I objectives that are slightly more stringent than those for the *ATF*. For 1-watt DR6 operation, where C/I ratios for DR6 with ATF are available only for systems in the TH series, the use of DF-LPF does not degrade the relative interference environment.

Four-Level Spectral Shaping: Summary. Performance measures for the 4-level, 22.631-MHz memory-based digital filter were summarized in the paragraphs above. Those measures—which include theoretical and measured power spectral densities, digital eye closure, BER-versus-S/N data, equipment signature curves, and RF spectral measures—attest to attainments at least as good as those achieved with advanced analog filter technology, especially when the short development interval and inherent reproducibility are considered.

The digital filter and LPF design is expedited by using a series of computer programs developed for this application. The programs first automatically measure and then merge the ARF and candidate LPF transfer functions. For independent values of α, pulse functions $p'(t)$ are then derived by:

1. Removing linear phase from $L(f)\,R(f)$, equivalent to a shift in the time domain
2. Normalizing that transfer function to 0 dB at 0 Hz
3. Introducing varying amounts of truncation.

For each pulse thus obtained, the PEC_M is theoretically computed. With α bounded by $0.35 \leq \alpha \leq 0.5$, the process is completed in just several minutes of central processing unit (CPU) time.

Eight-Level Spectral Shaping. The preceding sections focused on design considerations and performance attainments associated with spectral shaping transmitted 4-level signals. Because digital radio systems are migrating toward higher levels of QAM, and because successful designs for that situation illustrate approaches not exploited in the preceding example, we offer now an example of an 8-level filter, a more rigorous test of this filter approach. The greater challenge arises from the use of a longer pulse function stored in memory and longer digital words for signal representation. The necessity for a longer pulse follows from the observation that peak digital eye closure scales linearly with M, while memory requirements for the longer sampled pulse grow exponentially.

Analog receiver filter. Unlike the ARF used in the 4-level case, the receiver filter for the 8-level system was specifically designed for this example. The raised cosine roll-off is approximately 45 percent, the symbol rate is

Table I. *C/I* Objectives, dB, for Operation with the AT&T DR6 Radio System for ATF (or DF-LPF)

Foreign system*	Carrier separation (MHz)				
	0	7.5	15	22.5	30
TM-600	54 (55)	54 (55)	49 (50)	20 (24)	20 (20)
TM-900	59 (60)	59 (59)	56 (56)	34 (35)	20 (20)
TM-1200	63 (63)	62 (62)	60 (59)	40 (45)	20 (21)
TM-1200	73 (73)	72 (72)	69 (69)	48 (49)	23 (30)
NW-1200	73 (73)	72 (72)	69 (69)	49 (50)	34 (30)
TH-1800	79 (79)	77 (77)	76 (76)	69 (69)	37 (42), 42 (41)†
TH-1860	81 (74)	79 (79)	78 (78)	70 (70)	37 (42), 42 (41)†
TH-2400	79 (79)	76 (77)	76 (77)	74 (75)	50 (51), 50 (51)†
TH-18DV	79 (79)	77 (77)	76 (76)	69 (69)	37 (42)
TH-24DV	79 (79)	76 (77)	76 (77)	74 (75)	50 (51)
Video	64 (64)	64 (64)	57 (57)	42	36
Single sideband	64 (65)	64 (65)	64 (65)	64 (65)	46 (47)
DR6-30	65 (65)	64 (63)	61 (60)	54 (53)	29 (29)
RDS	65 (65)	68 (68)	68 (67)	66 (66)	61 (62)
NEC 16-QAM	65 (65)	65 (62)	61 (58)	56 (53)	45 (40)
Vidar	65 (67)	66 (64)	57 (59)	43 (43)	20 (22)

*These radio systems are more fully described in Reference 11. †DR6 at 1 W.

15.088 Mbaud, and the analog design approach is similar to that described in the discussion of the ARF under "Four-Level Spectral Shaping."

Low-pass filter. From the section "LPF Design Considerations," we note that the simple LPF requires redesign for each application that uses a significantly different half-Nyquist stopband. To avoid excessive distortion, the LPF cutoff, f_c, is placed within the stopband, which, for the present baud rate and 45 percent roll-off, is approximately 10.9 MHz $\leq f_{sb} \leq$ 15.1 MHz. The LPF is again a fifth-order Chebyshev design with 0.025-dB peak-to-peak ripple, the high-frequency cutoff is now f_c = 12 MHz (observe that f_c lies within f_{sb}), a single transmission zero occurs at 19.3 MHz, and the minimum stopband response is –42 dB.

Derivation of the digital filter pulse function. As before, LPF and receiver filter transfer functions were obtained by direct measurement, followed by creation of a computer file that stored the composite result after removing flat loss at 0 Hz. Unlike the 4-level example, however, the receiver filter was designed specifically for this case. In particular, special effort was made to hold the phase as linear as possible over the frequency range for which there was a significant amplitude response (out to approximately 9 MHz). Experience has shown that a more symmetric (even) transmitter pulse better lends itself to truncation (i.e., tends toward smaller eye closure for an equivalent pulse length) than those that are notably asymmetric.

The measured composite response, with equation (2), yields a filter transfer function, $P(f)\,G(f)$, that provides a full-Nyquist channel. For $\alpha = 0.45$, with $p'(t)$ defined by 18 samples, the PEC for an 8-level signal was computed as 15.0 percent (the corresponding eye

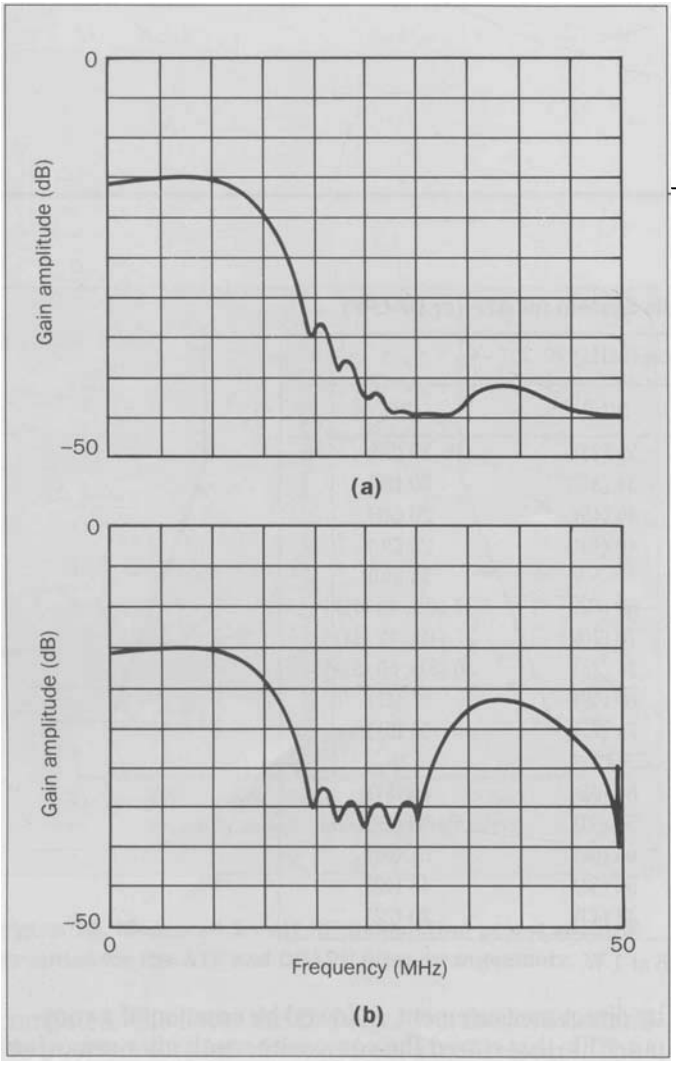

Figure 11. Transmitted amplitude spectrum measured (a) with and (b) without LPF.

closure for a 4-level signal would be 6.4 percent), a performance measure competitive with that attained by using sophisticated analog technology. The theoretical end-to-end transfer function, $P'(f)\,G(f)\,L(f)\,R(f)$, was computed and compared with the ideal Nyquist function, $N(f, \alpha = 0.45)$; both the amplitude and phase characteristic attested to a spectral match superior to that achieved in the 4-level example.

Memory size and digital word length. The prototype filter was constructed by storing in memory signal values based on 18 $T/2$-spaced samples of the impulse function. Were the two-ROM architecture of Figure 1 again used, each ROM would be addressed by a 27-bit word and would require 134,217,728 memory locations. Since memory of that size is impractical with today's technology, the address was segmented into three 9-bit words, and the partial-sum ROMs were augmented with two intermediate adders.

In addition, precision was enhanced by representing the memory output by 12 bits and retaining 10 bits of accuracy through the adders, which were followed by 10-bit A/D conversion. The 12-bit output from each unit of a functional memory pair (the two outputs within each symbol period) was actually accomplished by three ROMs, each with an 8-bit output. Two ROMs provided the 8 most significant bits for two outputs; the 8-bit output from the third ROM was split into two 4-bit words, each providing the 4 least significant bits in the desired 12-bit signal representation.

Eight-Level Shaping Performance. As before, the truncated impulse response was used to compute the output for each of the unique addresses to the nine ROMs required in the filter (three sets of partial-sum ROMs, each set made up of three ROMs for the expanded word length). The signals were scaled so that no symbol sequence could cause overflow in the composite adders or D/A converter.

Spectra. The transmitted amplitude spectrum was measured with and without the LPF, and appears in Figure 11. While not presented here, a comparison of the measured synthesizer output, without the LPF filter, shows excellent agreement with theoretical data (also, see Reference 3). In addition, Figure 11 indicates that the LPF provides a transfer function that eliminates the periodic portion of the spectrum without significantly affecting the baseband portion. In this case, the LPF first exhibits a discernible effect near 13.5 MHz, where the transmitted shape is already down –40 dB.

Digital Eyes and BER versus *S/N*. Digital eye measurements appear in Figure 12. The data of this figure apply to two cases: an analog transmitter and receiver

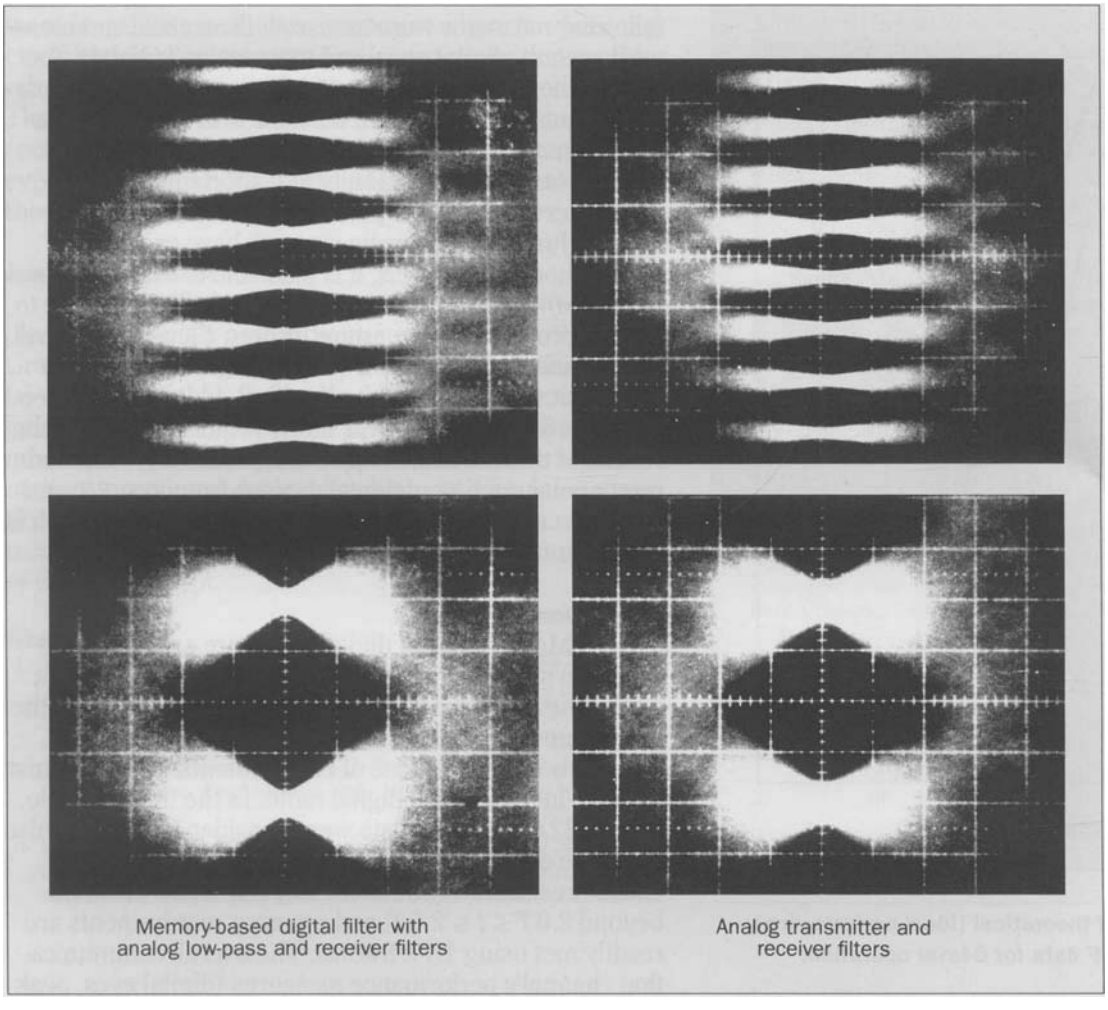

Figure 12. Measured 8-level digital eyes: those on the left correspond to the DF-LPF-ARF combination; those on the right to an analog filter pair.

filter pair (early feasibility models for a 64-QAM 22.6-Mbaud radio system[12]) and the DF-LPF complementing the ARF previously described. The different performance measures are qualitatively evident, with the former case corresponding to an eye closure of 18.5 percent and the latter case, 11.7 percent. The measured 11.7 percent value compares favorably with the theoretical 15.0 percent, especially since the measured data do not reveal eye closure peaks.

BER-versus-S/N measurements were made by techniques similar to those described under "Digital Eye Closure and BER versus S/N" for 4-level shaping. Figure 13 compares theoretical (ideal) performance with that measured using the DF-LPF-ARF configuration. The

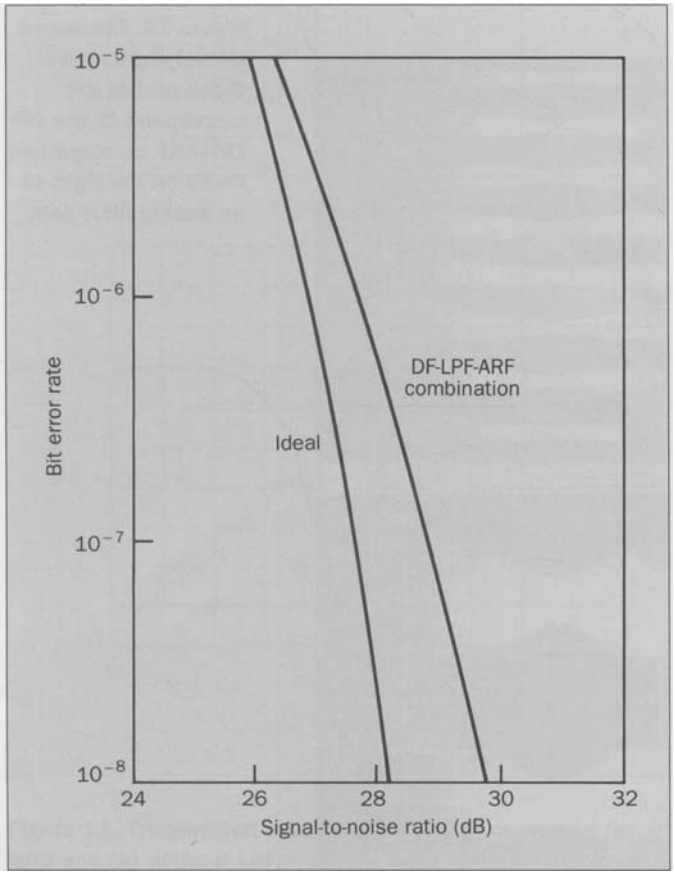

Figure 13. Comparison of theoretical (ideal performance) and measured DF-LPF-ARF data for 8-level operation.

figure reveals that the experimental 8-level data are quite similar—relative to ideal performance—to that measured for the 4-level DF-LPF-ARF case.

Eight-Level Spectral Shaping: Summary. The material above reviewed the design approach and performance capabilities for an 8-level digital filter that makes use of partial-sum memory units and expanded output word length. For this 15.088-Mbaud example, the following measures were assessed: theoretical and measured spectra, digital eyes, and BER-versus-S/N data. As before, the transmitter filter exhibits capabilities comparable, if not superior, to that attained with advanced analog means. Again, this digital approach offers inherent manufacturing reproducibility and shortened development intervals, with the potential for less cost.

Just as digital radio systems have evolved to higher modulation levels, it is plausible to expect 16-level (256-QAM) systems to become economically attractive to service providers in the future. Where 4-level and 8-level modulation required 10-bit (5 samples, 2 bits/symbol) and 27-bit (9 samples, 3 bits/symbol) addresses, respectively, a 16-level system will surely require more. Yet the results of this section, coupled with declining costs and power consumption of digital devices (memory, S/P and D/A converters, SR), suggest that this general approach is viable for future radio systems.

Conclusion

Memory-based digital filters are an efficacious means to shape transmitted data signals. After giving a brief review of basic principles, we have documented the performance attainments of this technology for the extremely important case of complementary half-Nyquist filtering in high-speed digital radio. In the first example, 4-level, 22.631-Mbaud data were considered. The impulse response of the desired spectrally shaped transmitted data were accurately described by impulse truncation beyond $2.0T \leq t \leq 2.5T$, and memory requirements are readily met using $1K \times 8$ ROMs. The overall communication channel's performance measures (digital eyes, peak eye closures, BERs, and multipath signatures) are competitive with sophisticated analog filter pairs. The memory-based digital filter offers the benefits of reduced size, less cost, inherent reproducibility, and a shortened development interval.

The second design example is, in several respects, more significant than the first. For the 8-level case, the dual approaches of address segmentation and

word length expansion are important adjuncts where precise filtering requires stored pulse functions that would otherwise be impractical with today's digital technology. The digital filter is again used to complement an analog receiver filter and provide a communication channel with eye closures and BERs comparable to those of state-of-the-art analog methods.

Acknowledgments

The authors are pleased to cite the following people for their timely and enthusiastic assistance: R. R. Grady for providing computer tools for simulation of digital radio systems; J. P. MacEachern for laboratory assistance (model fabrication and performance measurements); and H. C. Reeve for special insight into aspects of the supporting software development. Special recognition is also given to anonymous reviewers whose comments have significantly improved the content and style of this manuscript.

References

1. W. Debus, T. L. Osborne, and C. A. Siller, Jr., "Digital Synthesis Technique Having Predetermined Time and Frequency Domain Characteristics," U.S. Patent 4,710,891, December 1, 1987.
2. C. A. Siller, Jr. and W. Debus, "Spectral Shaping of M-State Signals for Bandlimited Communications," *Proceedings of International Communications Conference*, Seattle, Washington, June 1987, pp. 49.4.1-49.4.8.
3. C. A. Siller, Jr., W. Debus, and T. L. Osborne, "Spectral Shaping and Digital Synthesis of an M-ary Data Time Series," *IEEE Communications Magazine*, Vol. 27, No. 2, February 1989, pp. 15-24.
4. A. Peled and B. Liu, "A New Hardware Realization of Digital Filters," *IEEE Transactions on Acoustics, Speech, and Signal Processing*, Vol. ASSP-22, No. 6, December 1974, pp. 456-462.
5. R. M.-M. Chen et al., "L5 Coaxial-Carrier Transmission System: Role of Computing and Precision Measurements," *Bell System Technical Journal*, Vol. 53, No. 10, December 1974, pp. 2249-2269.
6. P. R. Chevillat and G. Ungerboeck, "Optimum FIR Transmitter and Receiver Filters for Data Transmission over Band-Limited Channels," *IEEE Transactions on Communications*, Vol. COM-30, No. 8, August 1982, pp. 1909-1915.
7. J. J. Kenny, "Digital Radio for 90-Mb/s, 16-QAM Transmission at 6 and 11 GHz," *Microwave Journal*, August 1982, pp. 71-80.
8. M. Schwartz, *Information Transmission, Modulation, and Noise*, McGraw-Hill, New York, 1980.
9. W. D. Rummler, "A New Selective Fading Model: Application to Propagation Data," *Bell System Technical Journal*, Vol. 59, No. 5, May-June 1979, pp. 1037-1071.
10. "Code of Federal Regulations: Telecommunications (47)," Part 21.106, Federal Communications Commission, revised October 1, 1987, pp. 38-39.
11. "DR6-30/DR11-40 Digital System—System Application Engineering," *Bell System Practices*, AT&T Standard, Section 421-200-141, Issue 2, October 1982, p. 38. (Available from AT&T Network Systems Customer Information Center, phone 1-800-432-6600.)
12. C. P. Bates, W. G. Robinson, and M. A. Skinner, "DR6-30-135 System Design and Application," *Proceedings of Global Communications Conference*, Atlanta, Georgia, November 26-29, 1984, pp. 16.7.1–16.7.8.

(Manuscript received March 26, 1990)